Int. J. Electrochem. Sci., 16 **(2021)** Article ID: 210831, doi: 10.20964/2021.08.22

International Journal of
ELECTROCHEMICAL
SCIENCE
www.electrochemsci.org

Microstructures, Magnetic and Electrical Properties of $BaFe_{12}O_{19}$/ZnO Composite Material

Perdinan Sinuhaji[1], Masno Ginting[2,], Perdamean Sebayang[2,*], Martha Rianna[1], Muhammadin Hamid[1], Tua Raja Simbolon[1], Veryyon Harahap[1,4], Anggito P.Tetuko[2], Eko Arief Setiadi[2], Nining S. Asri[2], Lukman Faris Nurdiyansah[2], Achmad Maulana Soehada Sebayang[3]*

[1] Universitas Sumatera Utara, Medan 20155, Indonesia
[2] Research Center for Physics, Indonesian Institute of Sciences (LIPI), Tangerang Selatan, Banten 15314, Indonesia
[3] Department of Mechanical Engineering, Universitas Pamulang, Tangerang Selatan, Banten, 15314, Indonesia
[4] Universitas Efarina, Pematang Siantar, Sumatera Utara 21162, Indonesia
[*]E-mail: masno.ginting@lipi.go.id; perdamean.sebayang@lipi.go.id

Received: 1 May 2021 / *Accepted:* 5 June 2021 / *Published:* 30 June 2021

The composite material of $BaFe_{12}O_{19}$/ZnO has been fabricated via the solid-state reaction technique with calcination temperature at 900°C for 4 h. The mixing and the milling processes were conducted using High Energy Milling (HEM) for 3 h in a toluene medium. The optimal condition of the sample $BaFe_{12}O_{19}$/ZnO was attained with the composition of 50:50 wt%. The XRD analysis revealed the emerging of two phases occurs including $BaFe_{12}O_{19}$ (the primary phase) and ZnO (the secondary phase). Additionally, the SEM images confirmed that the particles of the composite were granulated with average particle sizes of 3-5 µm. While the VSM examination showed that the Zn addition as a composite material decreased the magnetic properties. Moreover, the I-V measurments showed that nonlinear line increased with the addition of ZnO as a composite material in $BaFe_{12}O_{19}$/ZnO. Tge optimum magnetic properties was obtained for $BaFe_{12}O_{19}$/ZnO presented in the following: Ms = 39.91 emu g^{-1}, Mr = 22.61 emu g^{-1}, Hc = 2917 Oe, respectively. From the electromagnetic characteristics were obtained that the $BaFe_{12}O_{19}$/ZnO composite material is suitable for a candidate as the micro-wave absorber.

Keywords: $BaFe_{12}O_{19}$, Solid State Reaction, Micro-structures, Magnetic Properties; Composite Material

1. INTRODUCTION

Barium hexaferrite ($BaFe_{12}O_{19}$) is a hard magnetic material, which is based on iron oxide [1]. Barium hexaferrite has high saturation magnetization and coercivity, high Curie temperature, low cost,

and high stability [2]–[4]. When the tetra-valence, di-valence of non and magnetic cations, ie: Al, Mg, Mn, Ni, Co, Ti, and Zn cations are substituted into the crystal lattice of barium hexaferrite, the obtained materials have magnetic and chemical properties [5], [6].

Tang et al [7] have conveyed regarding the manufacture of barium hexaferrite composite coated with ZnO particles and calcined at the temperature of 450^{o}C for 1 h using the co-precipitation method. The outcomes revealed that the crystal size of barium hexaferrite decrease with the addition of ZnO. Next, $BaFe_{12}O_{19}$/ZnO composites were fabricated by Jiang et al [8] using the sol-gel method. The results presented that the ZnO in the barium hexaferrite composite decreased the magnetization saturation value, thus could be used as a candidate for microwave absorber material [9]. Huang et al [10] reported the particle size of ZnO in graphite/ cobalt zinc ferrite composite is 5-10 μm with the graphite of 10 wt%. Further, the study by Nuraini et al [11] showed that the substitution of Zn did not change the crystal structure of barium hexaferrite. The synthesis of $BaFe_{12}O_{19}/Fe_3O_4$ nano-composite was conducted by Molaei [12], the results that magnetic properties decrease with the use of calcination temperature at 900^{o}C. Tyagi et al [13] reported the $BaFe_{12}O_{19}/ZnFe_2O_4$ particles had hexagonal plate shapes. The effect of zinc and nickel as composite could increase in the result of microwave properties from the result of barium hexaferrite particle [14, 15].

In this present work, barium hexaferrite ($BaFe_{12}O_{19}$) and zinc oxide (ZnO) powders were synthesized through the solid-state reaction technique calcined at 900^{o}C and 4 h holding time. Further, this work also examines the effects of ZnO addition on the characteristic of $BaFe_{12}O_{19}$.

2. EXPERIMENTAL

The composite material of Barium hexaferrite ($BaFe_{12}O_{19}$) / zinc oxide (ZnO) powder was fabricated via the solid-state reaction technique. The raw materials were $BaFe_{12}O_{19}$ technical and ZnO powder obtained from Sigma-Aldrich, Germany. $BaFe_{12}O_{19}$ and ZnO with a mass ratio (%) of 100:0. 50:50, and 0:100 were mixed using High Energy Milling (HEM) for 3 h in a toluene (15 ml) medium with the milling ball and the powder ratio was 10:1 or 10 gr of samples powders with 100 gr milling ball. After milling process, samples separated by spatula from milling ball and samples input to beaker glass (500 ml). After that, the samples was then dried in an oven at 100^{o}C for 24 hours to reduce H_2O for making powder. Then, the powder were grind the mixtures together in an agate mortar, they were placed in a 30-mL platinum crucible within a resistive furnace. The powder was calcined at 900^{o}C for 4 h with a heating/cooling rate of 10°C/min. The densities of the $BaFe_{12}O_{19}$/ ZnO powder at different compositions were measured according to Archimedes' principle. The powder of $BaFe_{12}O_{19,}$ ZnO, and $BaFe_{12}O_{19}$/ZnO composite material at different compositions were characterized by X-ray Diffraction using Cukα radiation (λ = 1.5406 Å), diffractometer (40 kV, 30 mA), Smartlab-Rigaku to investigate the crystal structure, Vibrating Sample Magnetometer (VSM250 Dexing Magnet Ltd) to study the magnetic property, and Scanning Electron Microscopy (JEOL) to observe the morphology and particles. I-V measurments using FLUKE 8842A Multimeter were used to analyze the electrical properties.

3. RESULTS AND DISCUSSION

The density of the $BaFe_{12}O_{19}$-ZnO composite powder at various compositions is shown in Figure 1. The measurement using Archimedes' principle suggested that the values are 5.21 g cm^{-3}, 5.38 g cm^{-3}, and 5.52 g cm^{-3}, respectively.

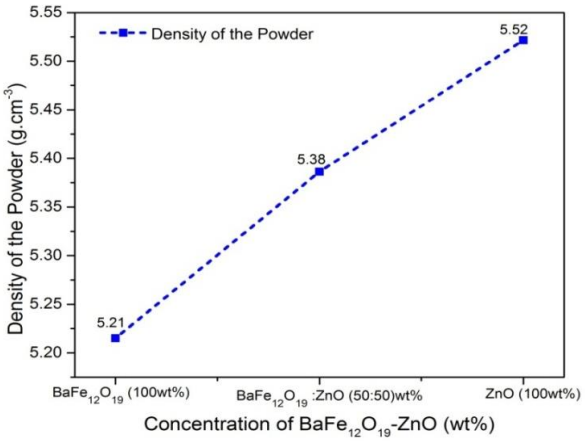

Figure 1. The density of the $BaFe_{12}O_{19}$/ZnO powder at different compositions of $BaFe_{12}O_{19}$/ZnO.

On the other hand, based on the reference, the theoretical density of $BaFe_{12}O_{19}$ and ZnO are 5.10-5.56 g cm^{-3} [16] and 5.60 g cm^{-3} [17]. The XRD patterns of $BaFe_{12}O_{19}$ (100 wt%), ZnO (100 wt%), and $BaFe_{12}O_{19}$/ZnO (50:50) wt% calcined at 900ºC for 4 h are shown in Figure 2.

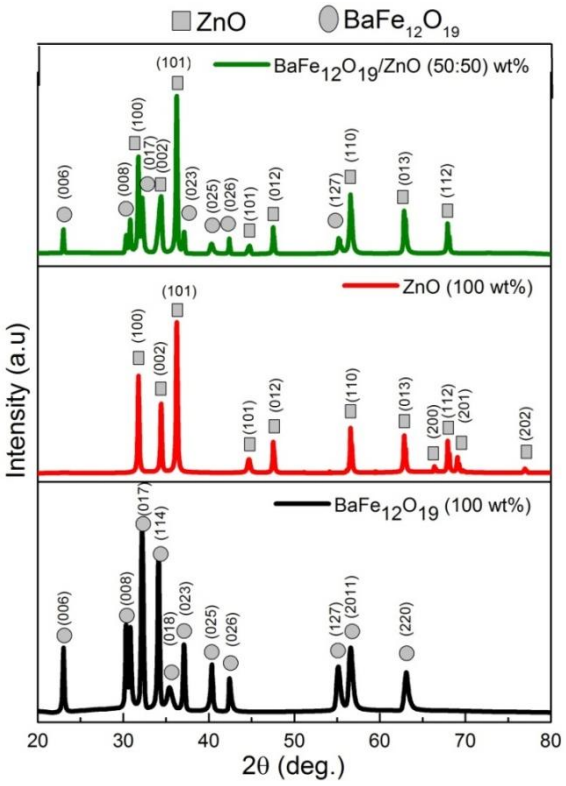

Figure 2. XRD Patterns : $BaFe_{12}O_{19}$ (100 wt%), ZnO (100 wt%), and $BaFe_{12}O_{19}$/ZnO (50:50) wt%

The XRD pattern of $BaFe_{12}O_{19}$/ZnO (50:50) wt% sample exhibits the emerging of two additional phases including the primary phase of $BaFe_{12}O_{19}$ and the secondary phase of ZnO. A previous study proposed that the composite of $BaFe_{12}O_{19}$/ZnO crystals was affected during the heating treatment process [18].

SEM-EDS and particle distributions histograms of $BaFe_{12}O_{19}$ (100 wt%) and $BaFe_{12}O_{19}$/ZnO (50:50) wt% analysis are displayed in Figure 3. It can be seen that the particles of the composite are granulated with average particle sizes of 5µm.

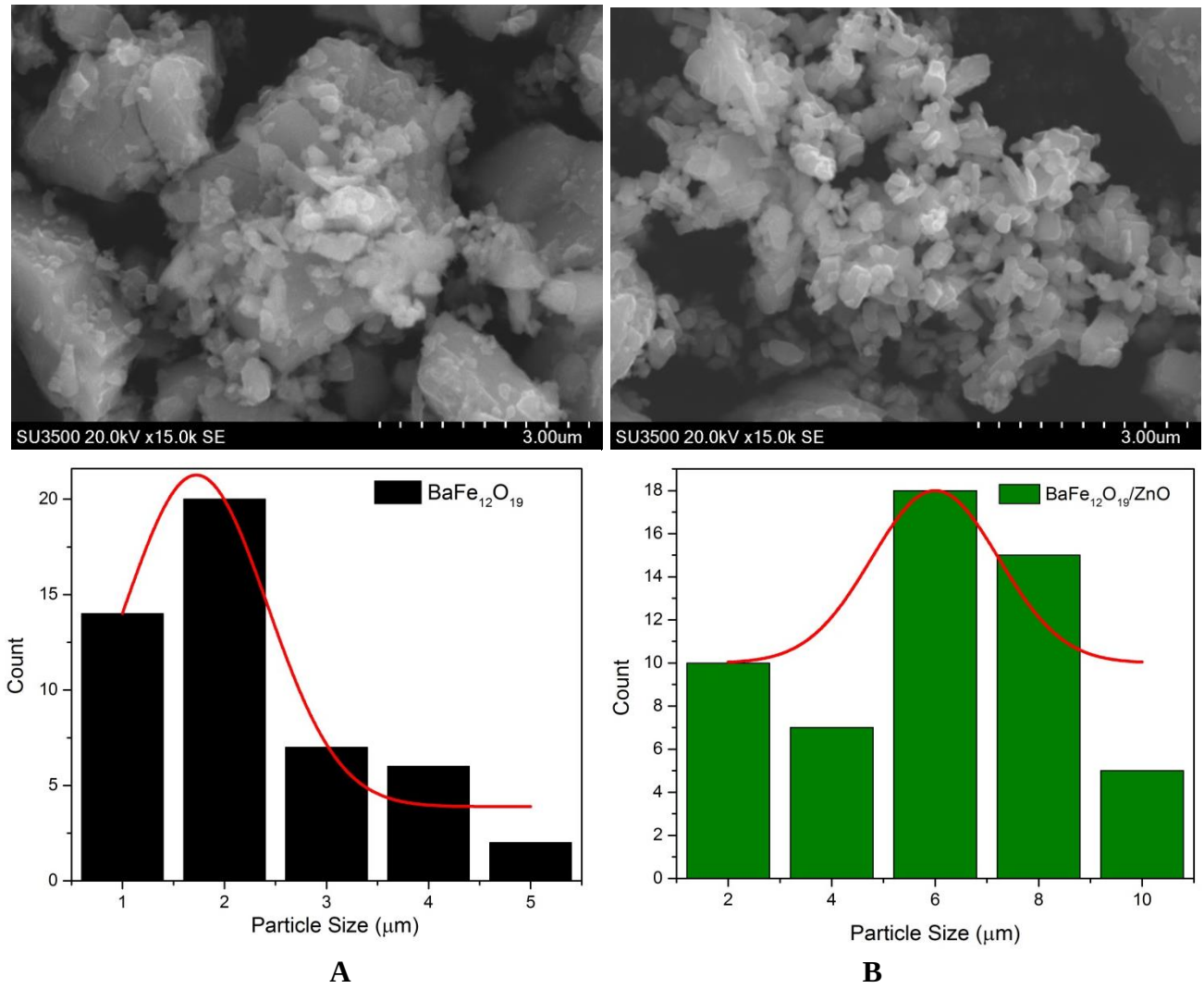

Figure 3. SEM images and Histograms of Particle Distributions of (a) $BaFe_{12}O_{19}$ (100 wt%), (b) $BaFe_{12}O_{19}$/ZnO (50:50) wt%

It appears that the greater the ZnO composition, the finer and smaller the surface morphology of the $BaFe_{12}O_{19}$/ZnO composites from Figure 3. This is closely related to the ZnO distribution in material composites of $BaFe_{12}O_{19}$/ZnO. $BaFe_{12}O_{19}$ has quite high magnetic properties so that $BaFe_{12}O_{19}$ and ZnO particles tend to form aggregates. The higher the ZnO composition, the aggregation between the $BaFe_{12}O_{19}$ grains will be decreased, so that the surface morphology of the

$BaFe_{12}O_{19}$/ZnO composite will appear smoother [19]. The presence of these granulated is caused by the calcination process at 900ºC as a result of the metal ions in the high energy milling process which indicates an enhanced alignment among grains [20]–[22].

Table 1 shows EDS analysis of $BaFe_{12}O_{19}$ and $BaFe_{12}O_{19}$/ZnO (50:50) wt% that denotes the existence of Ba, Fe, Zn, and O elements.

Table 1. EDS analysis of $BaFe_{12}O_{19}$ and $BaFe_{12}O_{19}$/ZnO (50:50) wt%

Sample	Element content			
	Ba (%wt)	**Fe (%wt)**	**Zn (%wt)**	**O (%wt)**
$BaFe_{12}O_{19}$	12.42	50.86	-	36.72
$BaFe_{12}O_{19}$/ZnO	3.47	36.80	27.41	32.32

Furthermore, based on the Table 1 EDS analysis of $BaFe_{12}O_{19}$ and $BaFe_{12}O_{19}$/ZnO (50:50) wt%, it is found that Fe is the largest element available compared to other elements in the material for both $BaFe_{12}O_{19}$ (100 wt%) and $BaFe_{12}O_{19}$/ZnO (50:50) wt%. The magnetic properties were studied using vibrating sample magnetometer at room temperature shown in Table 2, whereas hysteresis loop are shown in Figure 4.

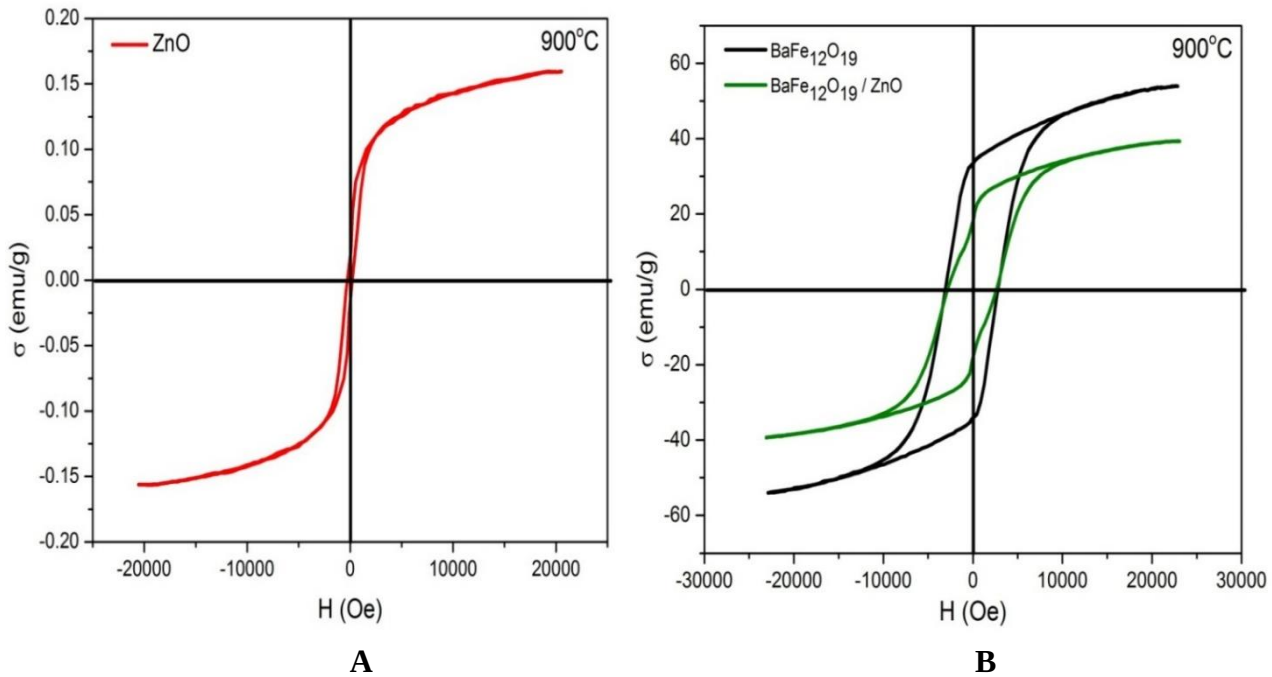

A **B**

Figure 4. Hysteresis Curve (a) ZnO (100 wt%), (b) $BaFe_{12}O_{19}$ (100 wt%) and $BaFe_{12}O_{19}$/ZnO (50:50) wt%

Table 2. Magnetic properties of $BaFe_{12}O_{19}$ and $BaFe_{12}O_{19}$/ZnO (50:50) wt% powder of samples

Sample	Magnetic Properties		
	Saturation, Ms (emu g^{-1})	**Remanence, Mr (emu g^{-1})**	**Coercivity, Hc (Oe)**
$BaFe_{12}O_{19}$	53.74	34.08	3280
ZnO	0.16	0.06	368
$BaFe_{12}O_{19}$/ZnO	39.91	22.61	2917

Based on the results in Figure 4 and Table 2, the addition of ZnO in the composite material of $BaFe_{12}O_{19}$/ZnO reduces the values of magnetic saturation (M_s), remanence (M_r), and coercivity (H_c), respectively. Therefore, it can be concluded that the addition of ZnO that has a diamagnetic behavior and a smaller magnetic moment declines the magnetic properties in the composite material of barium hexaferrite and zinc oxide [23]. Then, the electrical properties are closely related to the potential and current patterns of $BaFe_{12}O_{19}$/ZnO as shown in Figure 5, respectively.

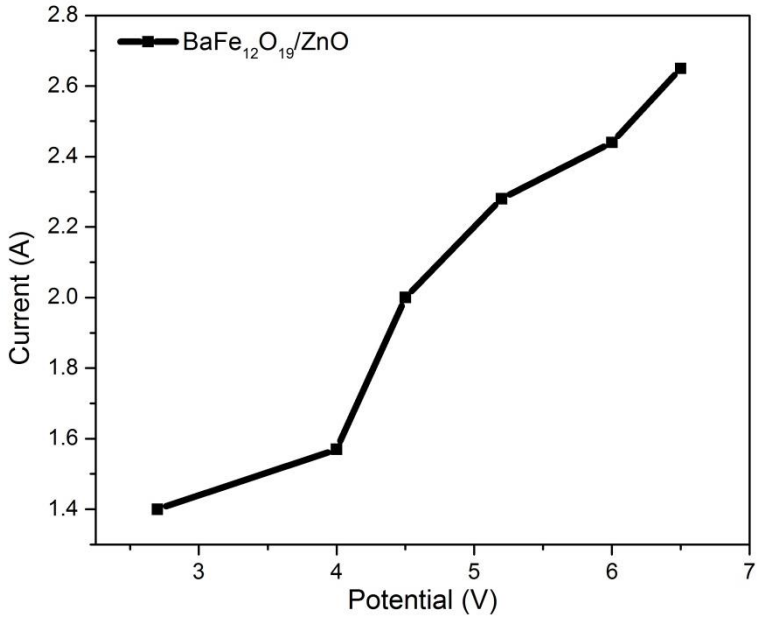

Figure 5. I-V curve of $BaFe_{12}O_{19}$/ZnO

Figure 5 displays the electrical properties of $BaFe_{12}O_{19}$/ZnO composite materials. The I-V curve was measured at a range of 2-7 Volt. Based on Figure 5, nonlinear line reversal current in the I-V curve increase with the addition of ZnO as a composite material in $BaFe_{12}O_{19}$. The experimental evidences to verify the ferroelectricity of $BaFe_{12}O_{19}$ ceramics has been studied Li et al [24]. Its also designates that current could be the improvement of oxygen kinetics properties and surface area of the electrode in $BaFe_{12}O_{19}$ after adding ZnO [25-26]. The sample of $BaFe_{12}O_{19}$/ZnO could be electrode

towards oxygen reduction because the peak intensities in the XRD patterns (Figure 2) have been decreased after adding ZnO as a composite in $BaFe_{12}O_{19}$. However, temperature calcination could be oxygen reduction in samples, so that the magnetic and electrical properties of the samples are affected, respectively.

This research aims to study the magnetic and electrical properties of all samples. Magnetic properties of high remanence could be potential in electromagnetic wave absorbers, component battery system, permanent magnetic material [27]. It points to that barium hexaferrite can be also applied to microwave absorption materials [22], [28]. In addition, this research exploited for magnetic and electrical properties results, it can be impacted for fabricating magnetic permanent material and electrochemical phenomena, respectively for applications of radar absorbing materials.

4. CONCLUSION

The analysis of the $BaFe_{12}O_{19}$/ZnO composite material fabricated via solid-state reaction technique at a temperature of 900ºC for 4 h has been declared. Based on the results, the optimal condition of the sample is achieved at $BaFe_{12}O_{19}$/ZnO (50:50) wt%. The XRD analysis reveals two phases of $BaFe_{12}O_{19}$ (the primary phase) and ZnO (the secondary phase). Meanwhile, the VSM analysis exhibits that the addition of Zn as the composite material decreases the magnetic properties in $BaFe_{12}O_{19}$/ZnO. The I-V measurments investigation further shows that nonlinear reversal current line in the I-V curve increase with the addition of ZnO as a composite material in $BaFe_{12}O_{19}$. The results show that $BaFe_{12}O_{19}$/ZnO composite material is suitable for a candidate as the micro-wave absorber material based on the electromagnetic characteristic.

ACKNOWLEDGMENTS
The authors thank to the Research Center for Physics, the Indonesian Institute of Sciences (LIPI), and Universitas Sumatera Utara for supporting this study.

References

1. P.G. Bercoff, H.R. Bertorello. *Mater. Sci. Forum.*, 302–303 (2009) 435–439.
2. M. El-Hilo, H. Pfeiffer, K. O'Grady, W. Schüppel, E. Sinn, P. Görnert, M. Röslerc, D.P.E. Dickson, R.W. Chantrell. *J. Magn. Magn. Mater.*, 129 (1994) 339–347.
3. Y. Liu, Y. Li, Liu Y. *Appl. Mech. Mater.*, 69 (2011) 6–11.
4. R.C. Pullar. *Prog. Mater. Sci.*, 57 (2012) 1191–1334.
5. E. Handoko, S. Iwan, S. Budi, B.S. Anggoron, A.M. Mangasi, M. Randa, J. Zulkarnain, C. Kurniawan, N.B.I. Sofyan, M. Alydrus., *Mater. Res. Express*., 5 (2018) 064003.
6. D.A. Vinnik, A.S. Semisalova, L.S. Mashkovtseva, A.K. Yakushechkina, S. Nemrava, S.A. Gudkovaa, D.A. Zherebtsov, N.S. Perovb, L.I. Isaenkod, R. Niewac. *Mater. Chem. Phys.*, 163 (2015) 416–420.
7. X. Tang, K. Hu. *Mater. Sci. Eng. B Solid-State Mater. Adv. Technol.*, 139 (2007) 119–123.
8. J. Jiang, L.H. Ai. *Phys. B Condens. Matter*,. 405 (2010) 2640–2642.
9. W. Chen, J. Zheng, Y. Li. *J. Alloys Compd.*, 513 (2012) 420–424.
10. X. Huang, J. Zhang, W. Rao, T. Sang, B. Song, C. Wong. *J. Alloys Compd.*, 662 (2016) 409–

414.
11. U. Nuraini, L. Amalia, K.C. Rosyidah, M. Zainuri. *Adv. Mater. Res.*, 1112 (2015) 19–22.
12. M.J. Molaei, A. Ataie, S.Raygan, M.R. Rahimipour, S.J. Picken, F.D. Tichelaar, E. Legarra, F.Plazaolae. *Mater. Charact.*, 63 (2012) 83–89.
13. S. Tyagi, V. S. Pandey, S. Goel, A. Garg. *Integr. Ferroelectr.*, 186 (2018) 25–31.
14. S. Sugimoto; S. Kondo, K. Okayama, H. Nakamura, D. Book, T. Kagotani, M. Homma. H. Ota, M. Kimura, R. Sato. *IEEE Trans. Magn.*, 35 (1999) 3154–3156.
15. H.S. Cho, S.S. Kim. *Ceram. Int.*, 45 (2019) 9406–9409.
16. R. Nowosielski, R. Babilas, G. Dercz, L. Pajk, J. Wrona. *Arch. Mater. Sci. Eng.*, 28 (2007) 735–742.
17. H. Morkoç and Ü. Özgür, *Zinc Oxide: Fundamentals, Materials and Device Technology*. 2009.
18. A. Rezaei, J. Saffari, G. Nabiyouni, D. Ghanbari. *J. Mater. Sci. Mater. Electron.*, 28 (2017) 6607–6618, 2017.
19. A. Rezaei, G. Nabiyouni, D. Ghanbari. *J. Mater. Sci. Mater. Electron.*, 27 (2016) 11339–11352.
20. R.P. Garcia, A. Delgado, Y. Guerra, B.V.M. Farias, D. Martinez, E. Skovroinski, A. Galembeck, E.P. Hernández. *Phys. Status Solidi Appl. Mater. Sci.*, 213 (2016) 2485–2491.
21. R. Gao. *Chinese Sci. Bull.*, 47 (2003) 1166.
22. M.J. Molaei, A. Ataie, S. Raygan, S.J. Picken. *Mater. Charact.*, 101 (2015) 78–82.
23. S. R. Janasi, M. Emura, F.J.G. Landgraf, D. Rodrigues. *J. Magn. Magn. Mater.*, 238 (2002) 168–172.
24 Xue Li, Guo-Long Tan. *J. Alloys Compd*., 858 (2021) 157722
25. X. Sun, L. Sheng, J. Yang, K. An, L. Yu, X. Zhao. *J. Mater. Sci. Mater. Electron.*, 28 (2017) 12900–12908.
26. R.D. Widodo, Priyono, Rusiyanto, S. Anis, R.I. Ilham, H.N. Firmansyah, N. Wahyuni. *IOP Conf. Ser.: Earth Environ. Sci.*, 700 (2021) 012001.
27. P. Jarupoom, P. Jaita, S. Manotham, T. Phatungthane, K. Chokethawai, C. Randorn, G. Rujijanagul. *J. Nanosci. Nanotechnol.*, 19 (2018) 1276-1282.
28. M. Delina, N. Nenni, W.A. Adi. *IOP Conf. Ser.: Mater. Sci. Eng.* 335 (2018) 012003.